Contribution from the Institute for Physical and Theoretical Chemistry, University of Frankfurt, Niederurseler Hang, 6000 Frankfurt am Main, FRG, and Institute for Inorganic Chemistry, University of Witten/Herdecke, 5810 Witten, FRG

Kinetics and Mechanism of the Iron(III)-Catalyzed Autoxidation of Sulfur(IV) Oxides in Aqueous Solution. 2. Decomposition of Transient Iron(III)–Sulfur(IV) Complexes

Jochen Kraft and Rudi van Eldik*

Received August 3, 1988

Mono-, bis-, and tris(sulfito) complexes of Fe(III), produced during the reaction of aquated Fe(III) and S(IV) oxides, undergo two successive redox reactions and produce Fe(II), SO_4^{2-}, and $S_2O_6^{2-}$. Spectrophotometric and kinetic measurements as well as ion chromatographic analyses of the reaction products were performed under the conditions $2.5 \times 10^{-4} \leq$ [Fe(III)] $\leq 6 \times 10^{-3}$ M, $5 \times 10^{-4} \leq$ [total S(IV)] $\leq 3 \times 10^{-2}$ M, $1.3 \leq$ pH ≤ 2.9, $13 \leq T \leq 40$ °C, and 0.1 M ionic strength. First-order rate constants for the first redox step are 0.14, 0.10, and 0.055 s^{-1} at pH = 2.5 and 25 °C for the tris-, bis-, and mono(sulfito) complexes, respectively. A pH dependence with a maximum rate constant at pH $\approx$ 2.2 was observed. The second redox step has a rate constant of 0.01 s^{-1} and exhibits only a slight pH dependence. Oxygen does not effect these steps but does initiate a more rapid redox reaction prior to the two steps mentioned before. It drastically affects the total amount of S(IV) oxidized to SO_4^{2-} and $S_2O_6^{2-}$. The mechanistic aspects of the reported data are discussed in reference to the suggested complex formation mechanism (part 1) and results reported in the literature.

Introduction

In part 1 of this series[1] we reported on a detailed study of the complex formation reactions between aquated Fe(III) and S(IV) oxides to produce Fe(III)–S(IV) transients. Evidence was presented for the formation of mono-, bis-, and tris(sulfito) complexes, depending on the pH and [total S(IV)] employed. The formation of two bis(sulfito) complexes (cis and trans) occurs within 5–10 ms after mixing. These species produce a common tris(sulfito) complex in a subsequent step within 200 ms. In this paper we report on the subsequent decomposition reactions of these Fe(III)–S(IV) transients that occur on a second and minute time scale. The rates of these reactions are such that they allow a detailed kinetic treatment based on spectrophotometrically determined rate plots as well as analyses of the reaction products employing spectroscopic and chromatographic techniques.[2]

Metal sulfito complexes, whether O- or S-bonded, undergo a variety of reactions, including substitution, aquation, isomerization (linkage and geometrical), and electron transfer.[3-19] These studies form a good basis for the interpretation of the results obtained in this investigation and assist the understanding of the unique role of Fe(III)–sulfito complexes in the catalyzed oxidation process.

Experimental Section

The employed experimental conditions, materials, preparation of solutions, instrumentation, rate measurements, and data-fitting procedures are similar to those adopted in part 1 of this series. In addition, a continuous-flow system was developed to record absorbance changes during the first 30–60 s after mixing. For this purpose two 100-cm^3 reservoir syringes (for the reactants) were connected to a 1 cm path length flow-through cell, which enabled the recording of a product spectrum ca. 100 ms after mixing. A Hewlett-Packard diode array spectrophotometer was used for this purpose. The Fe(III) concentration was monitored during the redox reactions by using sulfosalicylic acid to produce redox-stable Fe(III) complexes.[20] Aliquots of the reaction mixture (5 cm^3) were sampled at 20-s intervals for this purpose.

Product analysis was performed on a Sykam ion chromatograph using conductivity detection. The solvents were stored under He, which also prevented further oxidation of the injected sulfite solution during the analysis. The solvents were only in contact with inert Teflon or glass materials, except for the eluent, which was pumped by a stainless steel pump with ruby valves. Anion-exchange chromatography was used to separate and detect SO_3^{2-} and SO_4^{2-}. Phosphate (0.5 mM) as eluent at a flow rate of 1.5 cm^3 min^{-1} led to retention times of 2.7 and 8.8 min for these ions, respectively, with a low and stable eluent conductivity of 34 μS. Ion-pair chromatography was performed with a polystyrol/divinylbenzole polymer column, an eluent mixture consisting of 15% MeCN, 1 mM CO_3^{2-}, and 2.5 mM Bu_4NOH, and a flow rate of 1 cm^3 min^{-1}, enabling the separation and detection of $S_2O_6^{2-}$ and $S_2O_3^{2-}$ at retention times of 12 and 8 min, respectively. Thiosulfate was not detected in any of the investigated samples. The mixture of SO_3^{2-} and SO_4^{2-} was eluted as a single peak at 7.9 min.

* To whom all correspondence should be addressed at the University of Witten/Herdecke.

Results and Discussion

Spectroscopic Observations. The decomposition reactions of the Fe(III)–sulfito complexes can be followed conveniently by UV–vis spectrophotometry. A typical example of a repetitive-scan spectrum recorded during this reaction is given in Figure 13 (part 1). In contrast to our observations for the formation reactions, where the rate constants varied with the wavelength at which the reaction was studied, the absorbance–time plots and kinetic behavior are independent of wavelength. In general the kinetic plots clearly exhibit two consecutive reactions within the first 5–10 min of the decomposition process, followed by slower reaction steps on the time scale of hours, if measurements are performed under an Ar atmosphere (see Figure 1 in part 1). Although the lifetime of the transient complexes is such that it does not allow a complete identification, the spectral changes do enable a detailed kinetic analysis.

In an effort to obtain further information on the structure of the transient and product species, FT-IR spectra were recorded immediately after the formation reactions and during the decomposition process. The absorbances at 1080 and 1210 cm^{-1} increase in intensity during the decomposition reaction and shift to 1100 and 1240 cm^{-1}, respectively. This is ascribed to the partial formation of $S_2O_6^{2-}$ (1235, 1216, and 1102 cm^{-1}) and SO_4^{2-} (1104 and 981 cm^{-1}) during the reaction.[2]

The kinetic analysis of the reactions was supplemented by product analyses involving spectrophotometric determination of Fe(II/III) and ion chromatographic detection of SO_3^{2-}, $S_2O_6^{2-}$,

(1) Part 1: Kraft, J.; van Eldik, R. *Inorg. Chem.*, preceding paper in this issue.
(2) Kraft, J. Doctoral Dissertation, University of Frankfurt, 1987.
(3) van Eldik, R.; Harris, G. M. *Inorg. Chem.* **1980**, *19*, 880.
(4) van Eldik, R.; von Jouanne, J.; Harris, G. M. *Inorg. Chem.* **1982**, *21*, 2818.
(5) van Eldik, R. *Inorg. Chem.* **1983**, *22*, 353.
(6) Dash, A. C.; El-Awady, A. A.; Harris, G. M. *Inorg. Chem.* **1981**, *20*, 3160.
(7) El-Awady, A. A.; Harris, G. M. *Inorg. Chem.* **1981**, *20*, 1660.
(8) El-Awady, A. A.; Harris, G. M. *Inorg. Chem.* **1981**, *20*, 4251.
(9) Koshy, K. C.; Harris, G. M. *Inorg. Chem.* **1983**, *22*, 2947.
(10) Dasgupta, T. P.; Harris, G. M. *Inorg. Chem.* **1984**, *23*, 4399.
(11) Joshi, V. K.; van Eldik, R.; Harris, G. M. *Inorg. Chem.* **1986**, *25*, 2229.
(12) Moritzen, P. A.; El-Awady, A. A.; Harris, G. M. *Inorg. Chem.* **1985**, *24*, 313.
(13) El-Awady, A. A.; Harris, G. M. *Inorg. Chem.* **1986**, *25*, 1323.
(14) van Eldik, R. *Inorg. Chim. Acta* **1980**, *42*, 49.
(15) Spitzer, U.; van Eldik, R. *Inorg. Chem.* **1982**, *21*, 4008.
(16) Kraft, J.; van Eldik, R. *Inorg. Chem.* **1985**, *24*, 3391.
(17) Dash, A. C.; Roy, A.; Aditya, S. *Indian J. Chem.* **1986**, *25A*, 207.
(18) Mahal, G.; van Eldik, R. *Inorg. Chem.* **1987**, *26*, 1837.
(19) Mahal, G.; van Eldik, R. *Inorg. Chem.* **1987**, *26*, 2838.
(20) Müller, G. O. *Lehrbuch der Angewandten Chemie*; Hirzel Verlag: Leipzig, 1975; Vol. 3.

0020-1669/89/1328-2306$01.50/0

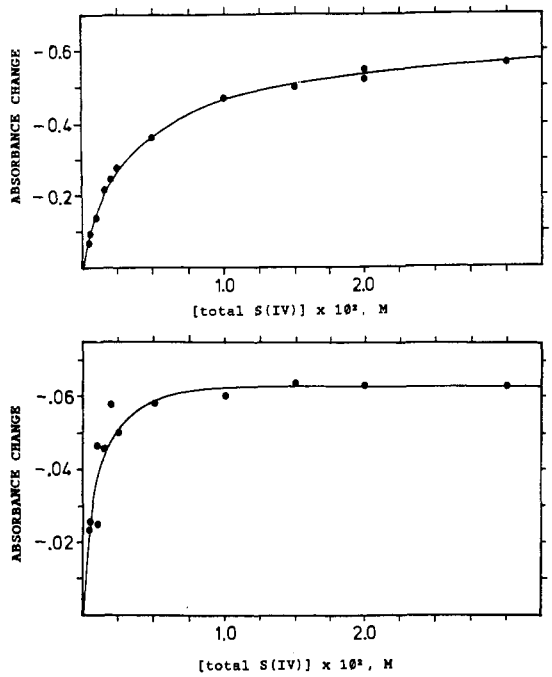

Figure 1. Absorbance change as a function of [total S(IV)] for steps III (upper plot) and IV (lower plot). Conditions: [Fe(III)] = 5×10^{-4} M, pH = 2.5, T = 25 °C, ionic strength 0.1 M, Ar atmosphere.

SO_4^{2-}, and $S_2O_3^{2-}$. For this purpose Fe(II) and Fe(III) can be complexed with sulfosalicylic acid and analyzed via the characteristic absorption bands. Due to the excess of sulfite used in the majority of experiments, analysis for Fe(II) proved to be inaccurate due to the subsequent formation of more Fe(II) as a result of the further decomposition of Fe(III)–sulfito species. For this reason Fe(III) was determined with sulfosalicylic acid in acidic medium,[20] whereby the subsequent redox reaction could be prevented. The absorbance at 505 nm (ϵ = 1790 M^{-1} cm^{-1}) was used to calculate the [Fe(III)] as a function of time during a kinetic run. These plots proved to be identical with those obtained directly from the spectral changes recorded in Figure 13 (part 1).

Kinetic Measurements and Product Distribution. Under most experimental conditions it was possible to separate the steps III and IV kinetically since the rate constants usually differed by a factor of 10. During the first step (III) the [Fe(III)] is reduced to ca. 10% of its original value at a 10-fold excess of sulfite. The absorbance decrease and associated rate constants at 390 nm exhibit similar trends (see Figures 1 and 2) for both steps (III and IV), with limiting rate constants of $(13.5 \pm 0.4) \times 10^{-2}$ and $(9.9 \pm 1.5) \times 10^{-3}$ s^{-1} at 25 °C, respectively. The [total S(IV)] dependence of the absorbance decrease can be associated with the different degrees of sulfite substitution achieved at different [total S(IV)] levels. The dependence of k_{obs} on this concentration (as noticed for step III) indicates that the different Fe(III)–S(IV) species exhibit different redox reactivities (varying between 0.055 and 0.135 s^{-1} at 25 °C depending on the number of sulfite ligands). In addition, step III is approximately 10 times faster than step IV, indicating that dimeric sulfito complexes may account for the slower redox process (IV). These observations should be complemented by the pH dependence of the process. The decrease in absorbance at 390 nm grows greater with increasing pH and reaches a limiting value at pH = 2.8 for step III, compared to an almost constant value with a slight increase at higher pH for step IV (see Figure 3). The associated rate constants exhibit a bell-shaped dependence on pH for step III, compared to a steady increase with pH for step IV (see Figure 4). Significant is the observation that Figure 4 indicates a bell-shaped pH dependence with a maximum rate constant at pH = 2.2. Similar findings were reported for the redox reactions of the O-bonded sulfito species $Co(tren)(H_2O)OSO_2^+$ and *trans*-$Co(en)_2(OSO_2)_2^-$[8,13] and were ascribed to the participation of two acid–base equilibria involving three complex species, of which one is significantly more redox

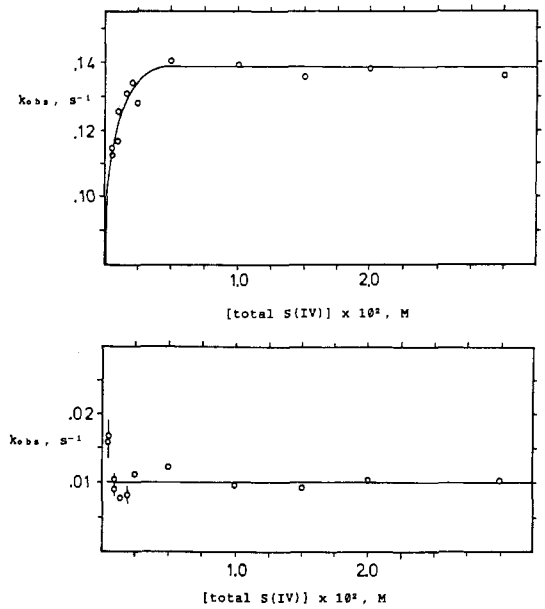

Figure 2. k_{obs} as a function of [total S(IV)] for steps III (upper plot) and IV (lower plot). Conditions: [Fe(III)] = 5×10^{-4} M, pH = 2.5, T = 25 °C, ionic strength 0.1 M, Ar atmosphere.

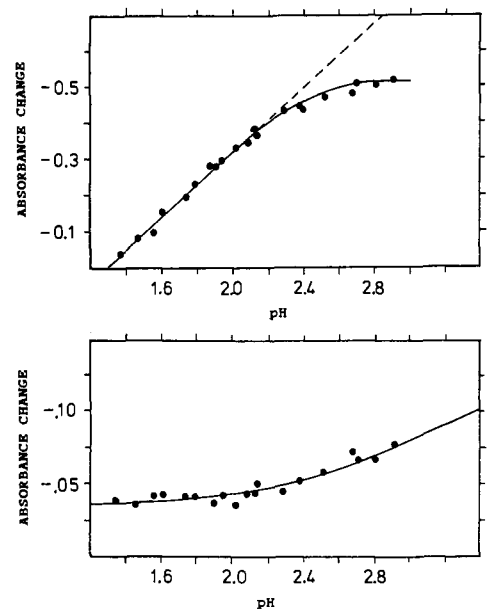

Figure 3. Absorbance change as a function of pH for steps III (upper plot) and IV (lower plot). Conditions: [Fe(III)] = 5×10^{-4} M, [total S(IV)] = 1×10^{-2} M, T = 25 °C, ionic strength 0.1 M, Ar atmosphere.

reactive than the other two. The completely different pH dependence observed for step IV (see Figure 3) is an indication that significantly different sulfito complexes participate in this redox step.

The speciation of the Fe(III)–sulfito complexes participating in steps III and IV can also be influenced by the [total Fe(III)] employed at a fixed pH and [total S(IV)]. The absorbance changes and associated rate constants observed under such conditions are summarized in Figures 5 and 6, respectively. Step III exhibits a linear increase in the absorbance decrease with increasing [total Fe(III)] to a maximum at ca. 1.5×10^{-3} M, changing to a slight decrease at higher concentrations. The corresponding rate constants decrease and reach a limiting value of $(5.4 \pm 0.4) \times 10^{-2}$ s^{-1} at ca. 1.5×10^{-3} M, under which conditions the mono(sulfito) complex should be the main species. In contrast, the absorbance decrease increases steadily with increasing [total Fe(III)] for step IV, accompanied by a slight increase in k_{obs} over the concentration range studied. These trends emphasize the difference in the nature of the complex species participating

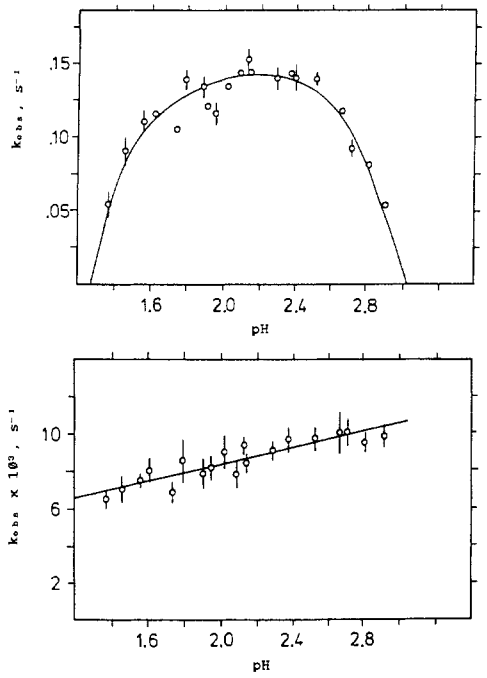

Figure 4. k_{obs} as a function of pH for steps III (upper plot) and IV (lower plot). Conditions: [Fe(III)] = 5×10^{-4} M, [total S(IV)] = 1×10^{-2} M, T = 25 °C, ionic strength 0.1 M, Ar atmosphere.

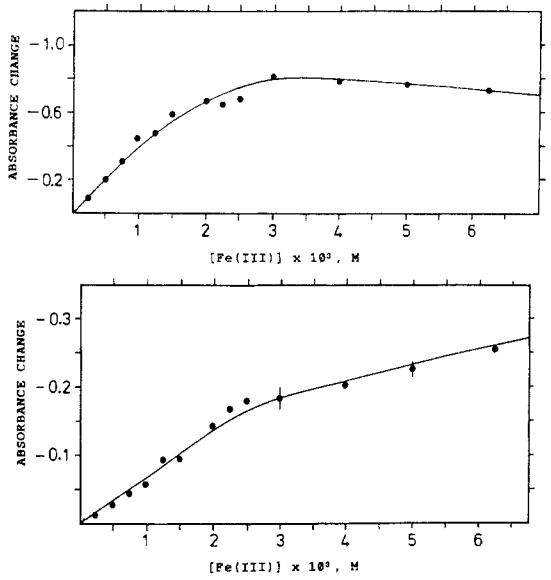

Figure 5. Absorbance change as a function of [Fe(III)] for steps III (upper plot) and IV (lower plot). Conditions: [total S(IV)] = 1.25×10^{-3} M, pH = 2.5, T = 25 °C, ionic strength 0.1 M, Ar atmosphere.

in these steps and underline the importance of their closer identification.

Another important piece of information on the nature of steps III and IV comes from the ion chromatographic analyses of the oxidation products formed under argonated conditions. The production of SO_4^{2-} and $S_2O_6^{2-}$ as a function of [total S(IV)], pH, and [total Fe(III)] is summarized in Table I. It follows from these data that the production of SO_4^{2-} decreases slightly with increasing [total S(IV)], increases significantly with increasing [total Fe(III)], and remains fairly constant as a function of pH. The $[S_2O_6^{2-}]$ increases with greater [total S(IV)] and with increasing pH. These trends give direct information on the nature of the redox processes and must be accounted for by the suggested mechanism.

Other kinetic parameters include $[O_2]$ and temperature, but before we discuss these it is appropriate to interpret the [total S(IV)], pH, and [total Fe(III)] dependencies reported above in terms of a suggested mechanism. Reactions III and IV occur on

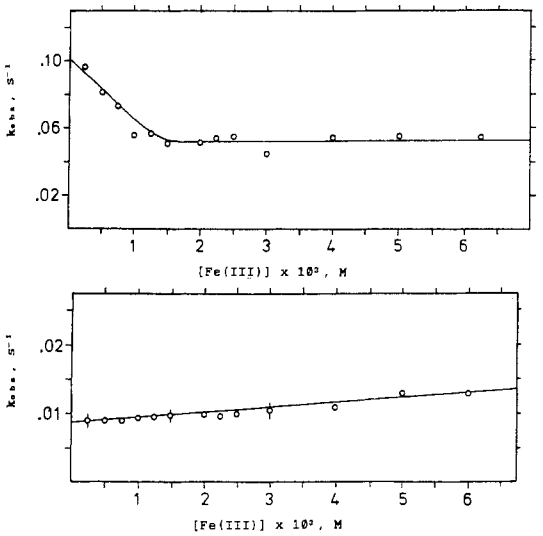

Figure 6. k_{obs} as a function of [Fe(III)] for steps III (upper plot) and IV (lower plot). Conditions: [total S(IV)] = 1.25×10^{-3} M, pH = 2.5, T = 25 °C, ionic strength 0.1 M, Ar atmosphere.

a time scale significantly slower than the formation steps I and II (see part 1 of this series), such that the latter can be considered as preequilibration steps, as summarized by reactions 1–6. As

$$Fe(H_2O)_5OH^{2+} + HSO_3^- \rightleftharpoons Fe(H_2O)_5SO_3^+ + H_2O \quad K_1 \quad (1)$$

$$Fe(H_2O)_5SO_3^+ \rightleftharpoons cis\text{-}Fe(H_2O)_4(SO_3)OH + H^+ \quad K_2 \quad (2)$$

$$Fe(H_2O)_5SO_3^+ + HSO_3^- \rightleftharpoons trans\text{-}Fe(H_2O)_4(SO_3)_2^- + H_3O^+ \quad K_3 \quad (3)$$

$$cis\text{-}Fe(H_2O)_4(SO_3)OH + HSO_3^- \rightleftharpoons cis\text{-}Fe(H_2O)_4(SO_3)_2^- + H_2O \quad K_4 \quad (4)$$

$$trans\text{-}Fe(H_2O)_4(SO_3)_2^- + HSO_3^- \rightleftharpoons Fe(H_2O)_3(SO_3)_3^{3-} + H_3O^+ \quad K_5 \quad (5)$$

$$cis\text{-}Fe(H_2O)_4(SO_3)_2^- + HSO_3^- \rightleftharpoons Fe(H_2O)_3(SO_3)_3^{3-} + H_3O^+ \quad K_6 \quad (6)$$

mentioned before,[1] the exact nature of the species produced in reactions 2–6, i.e., the coordination geometry of the sulfite ligand and the acid–base properties of coordinated water and sulfite, is unknown and the simplest possibilities are given in these reactions. The overall formation constant of the tris(sulfito) complex of ca. 1×10^7 M^{-3} brings about, at [total S(IV)] values of 10^{-2}, 5×10^{-3}, and 10^{-3} M, the ratios $[FeS_3]$:[Fe] = 10:1, 1.25:1, and 10^{-2}:1, respectively.

The [total S(IV)] dependence reported in Figures 1 and 2 (step III) fits the above trends. k_{obs} reaches a limiting rate at [total S(IV)] > 1×10^{-2} M, i.e., where practically all the Fe(III) is bound as the tris(sulfito) complex (FeS_3). At lower [total S(IV)] a significant contribution from the bis(sulfito) (FeS_2) species is expected to account for the lower redox reactivity. This can be expressed in a more quantitative way by the scheme in (7), where S = S(IV) oxide.

$$\begin{array}{ccc} Fe^{III}S_2 + S & \overset{K_7}{\rightleftharpoons} & Fe^{III}S_3 \\ {\scriptstyle k_1}\downarrow & & \uparrow{\scriptstyle k_2} \\ Fe^{II}S + S^{V/VI} & \longleftarrow & \end{array} \quad (7)$$

The first-order disappearance of these species results in (8), where $K_7 = K_5$ (=58 M^{-1}) or $K_7 = K_6$ (≥650 M^{-1}). At low [total

$$k_{obs} = \frac{k_1 + k_2K_7[\text{total S(IV)}]}{1 + K_7[\text{total S(IV)}]} \quad (8)$$

S(IV)], eq 8 reduces to $k_{obs} = k_1 + k_2K_7$ [total S(IV)], and at high [total S(IV)] eq 8 reduces to $k_{obs} = k_2$. The results in Figure

Table I. Distribution of the S–O Product Species during the Redox Decomposition Reactions as a Function of [Fe(III)], [Total S(IV)], and pH[a]

				reacn time, min		
				5		40
[Fe(III)], M	10^3[total S(IV)], M	pH	atmosphere	$10^3[SO_3^{2-}]$, M	$10^4[SO_4^{2-}]$, M	$10^4[S_2O_6^{2-}]$, M
5×10^{-4}	0.5	3.42	Ar		3.3 ● 0.2	
	1.0	3.30			3.2 ± 0.8	
	2.0	3.40			2.6 ± 0.5	
	3.0	3.48			2.6 ± 0.2	
	4.0	3.56			2.6 ± 0.8	
	5.0	3.47			2.6 ± 0.4	
5×10^{-4}	0.5	3.36	Ar			0.44
	1.0	3.41				0.85
	2.0	3.45				1.31
	3.0	3.54				1.78
	4.0	3.54				1.58
	5.0	3.52				1.62
5×10^{-4}	1.0	3.19	O_2			0.58
	2.0	3.01				1.67
	3.0	2.83				3.07
	4.0	2.71				3.52
0.5×10^{-3}	2.0	3.40	Ar	1.40	2.61	
1.0×10^{-3}		3.06		0.56	6.09	
1.5×10^{-3}		2.93		0.41	7.57	
2.0×10^{-3}		2.86		0.24	9.98	
0.5×10^{-3}	4.0	3.56	Ar	3.79	2.37	
1.0×10^{-3}		3.18		2.69	4.36	
2.0×10^{-3}		2.88		1.76	5.71	
3.0×10^{-3}		2.65		0.98	7.79	
0.5×10^{-3}	2.0	3.01	O_2			1.67
1.0×10^{-3}		2.93				3.11
1.5×10^{-3}		2.84				3.49
2.0×10^{-3}		2.70				4.30
0.5×10^{-3}	4.0	2.71	O_2			3.52
1.0×10^{-3}		2.80				5.99
2.0×10^{-3}		2.65				8.26
3.0×10^{-3}		2.54				9.44
5×10^{-4}	2	3.40	Ar		2.6	
		3.10			2.7	
		2.84			2.8	
		2.39			2.1	
		2.00			2.0	
5×10^{-4}	2	2.82	Ar			1.65
		2.38				1.22
		2.13				0.90
5×10^{-4}	2	2.22	O_2			0.95
		2.55				1.12
		2.70				1.45
		2.80				1.56
		2.87				1.65
		2.92				1.76

[a] T = 25 °C, ionic strength not adjusted.

2 suggest that $k_1 \approx 0.10$ s^{-1} and $k_2 = 0.14$ s^{-1} at 25 °C. The pH dependence of step III (Figures 3 and 4) suggest that two acid–base equilibria affect the redox reactivity of the tris(sulfito) complex. This can be formulated in a general way with the rate-determining electron-transfer step shown in (9).

$$Fe^{III}S_3H_2 \overset{K_8}{\rightleftharpoons} Fe^{III}S_3H \overset{K_9}{\rightleftharpoons} Fe^{III}S_3 \qquad (9)$$

$$\downarrow k_3$$

$$Fe^{II}S + S^{V/VI}$$

The rate law for such a scheme is given in (10), and a comparison with the experimental data in Figure 4 suggests[8,13] that $pK_8 \approx 1.4$, $pK_9 \approx 2.8$, and $k_3 \approx 0.14$ s^{-1} at 25 °C. Coordinated

$$k_{obs} = \frac{k_3K_8[H^+]}{K_8K_9 + K_8[H^+] + [H^+]^2} \qquad (10)$$

bisulfite ligands, whether O- or S-bonded, are expected to exhibit pK_a values significantly lower than for uncoordinated bisulfite, viz. 6.3 (see part 1), from which it follows that the values for pK_8 and pK_9 are very reasonable for coordinated bisulfite. Similar results were reported for Co(III) sulfito complexes.[8,13] S-bonded complexes are favored above O-bonded species, since the latter tend to lose SO_2 (via O–S bond cleavage) on acidification, which will decompose the complex rather than lead to electron transfer. The [Fe(III)] dependence of step III (see Figures 5 and 6) suggests that the mechanism in (7) can be extended to include the mono(sulfito) species ($Fe^{III}S$), which undergoes electron transfer at a rate of 0.05 s^{-1} (limiting value in Figure 6) at 25 °C. Comparison with the values of k_1 and k_2 quoted above indicates that the magnitude of the electron-transfer rate constant correlates directly with the number of sulfite ligands coordinated to the metal center, viz. 0.05, 0.10, and 0.14 s^{-1} for the 1:1, 1:2, and 1:3 complexes, respectively.

The [total S(IV)] dependence of step IV (see Figures 1 and 2) indicates that the reaction goes to completion at [total S(IV)] $\geq 5 \times 10^{-3}$ M, i.e., where complete formation of the tris(sulfito) species occurs. In addition the pH dependence of this step suggests a steady increase in k_{obs} on increasing pH (see Figures 3 and 4).

These trends can best be interpreted in terms of a redox process involving bridged bis- and tris(sulfito) complexes. The increase in k_{obs} with increasing pH suggests these to be hydroxo-bridged species or bridged species in which deprotonation leads to the formation of a more reactive species. These bridged species are significantly more stable (by a factor of ca. 10) than the monomeric complexes and represent up to 15% of the overall decomposition process. The [total Fe(III)] dependence reported in Figures 5 and 6 is also in line with the formation of bridged Fe(III) complexes under these conditions. The exact nature of these species is unknown, and realistic possibilities are $(SO_3)_2Fe(\mu\text{-}SO_3)_2Fe(SO_3)_2$, $(SO_3)_3Fe(\mu\text{-}OH)(\mu\text{-}SO_3)Fe(SO_3)_2$, $(SO_3)_3Fe(\mu\text{-}OH)_2Fe(SO_3)_3$, etc.

The formation of sulfate was monitored 5 min after the start of the reaction, i.e., almost toward the end of step IV. Similar analyses for $S_2O_6^{2-}$ indicated large fluctuations presumably due to subsequent redox reactions during the analytical procedure. Therefore, analyses for $S_2O_6^{2-}$ could only be performed after longer reaction times of between 30 and 40 min. At a constant [total Fe(III)], an increase in [S(IV)] causes a decrease in the $[SO_4^{2-}]$ accompanied by an increase in the $[S_2O_6^{2-}]$. This indicates that the formation of the tris(sulfito) species (reactions 5 and 6) favors the production of $S_2O_6^{2-}$, which is quite logical since electron transfer results in the formation of a sulfite radical, which can combine with the sulfite ligand in the cis position to eventually produce the $S_2O_6^{2-}$ species.

Series of experiments were performed to determine the influence of O_2 on the redox decomposition. An important observation is that in the presence of O_2 an additional step (IIIa) can be observed prior to steps III and IV observed in the absence of O_2. This reaction is also accompanied by a decrease in absorbance at 390 nm. The [total S(IV)] dependence of this decrease and the associated rate constants are summarized in Figure 7. Under limiting conditions step IIIa is ca. 4 times faster than step III. The above trends are interpreted in terms of the formation of oxo–sulfito complexes of the type $Fe(O_2)(SO_3)_{2/3}$, which undergo a fairly rapid redox reaction. The results in Table I demonstrate that the presence of O_2 markedly enhances the production of $S_2O_6^{2-}$ at high [total S(IV)]. The possible occurrence of two electron-transfer reactions on the oxo–bis(sulfito) and oxo–tris(sulfito) complexes, as outlined in (11), may account for the higher

$$Fe^{III}(S^{IV}O_3)_2 + O_2 \rightarrow (O_2)Fe^{III}(S^{IV}O_3)_2$$

$$(O_2)Fe^{III}(S^{IV}O_3)_2 \rightarrow (O_2)Fe^{II}(S^{IV}O_3)(S^{V}O_3)$$

$$(O_2)Fe^{II}(S^{IV}O_3)(S^{V}O_3) \rightarrow (^{-}O_2)Fe^{III}(S^{IV}O_3)(S^{V}O_3) \quad (11)$$

$$(^{-}O_2)Fe^{III}(S^{IV}O_3)(S^{V}O_3) \rightarrow (^{-}O_2)Fe^{II}(S^{V}O_3)_2 \xrightarrow{H^+} H_2O_2 + Fe(III) + S_2O_6^{2-}$$

$$\text{or} \rightarrow (^{-}O_2)Fe^{II}(S^{IV}O_3)(S^{VI}O_3) \xrightarrow{H^+} H_2O_2 + Fe(III) + SO_3^{2-} + SO_4^{2-}$$

production of $S_2O_6^{2-}$ via the combination of two SO_3^- species coordinated to the metal center. This scheme clearly demonstrates the catalytic effect of oxygen in reoxidation of the metal center. This cycle can be repeated several times, depending on the number of sulfite molecules coordinated to the metal center and the rate at which the SO_3^- species can be substituted by SO_3^{2-}. The oxygen molecule can in principle accommodate four electrons to oxidize four S(IV) oxides to S(V) or two S(IV) oxides to S(VI) species.

The participation of an oxo–sulfito–Fe(III) species in the autoxidation of S(IV) oxides was also suggested by Conklin and Hoffmann.[21] In their mechanism it is suggested that $Fe^{II}(OH)(OS^{V}O_2)$ reacts with O_2 to produce $(O_2^-)Fe^{III}(OH)(OS^{V}O_2)$, which subsequently produces $(O_2^{2-})Fe^{III}(OH)(OS^{VI}O_2)$ and decomposes in acidic medium to $FeOH^{2+}$, SO_3 (i.e., SO_4^{2-}), and H_2O_2. Furthermore, these suggestions are in line with the general finding[22] that metal peroxo complexes can react with SO_2 (or sulfite) to produce sulfato complexes or sulfate. In this respect it is important to note that the electron transfer from Fe^{II} to O_2 in such complexes is much faster in the presence of sulfite, i.e., when we are dealing with an Fe(II) sulfito complex.[23] Thus, Fe(II) sulfito complexes can catalyze the oxidation of Fe(II) to produce reactive Fe(III) centers.

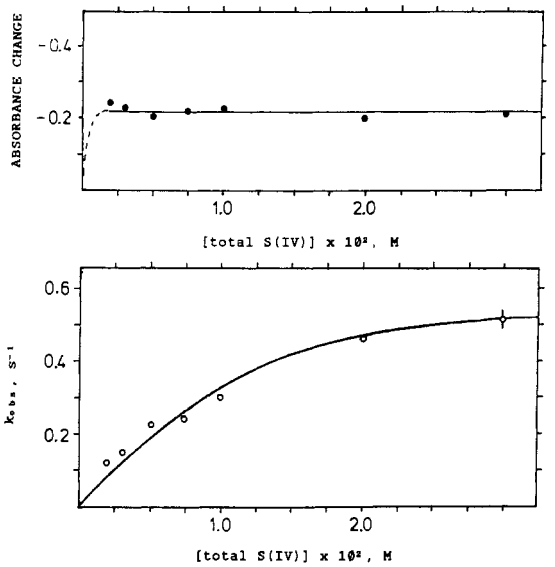

Figure 7. Absorbance change and k_{obs} as a function of [total S(IV)] for step IIIa. Conditions: [Fe(III)] = 5×10^{-4} M, pH = 2.5, T = 25 °C, O_2-saturated Fe(III) solution, ionic strength 0.1 M.

Further mechanistic information comes from the temperature dependence of steps III and IV (see Table II). For the given experimental conditions $\Delta H^{\ddagger}$(step III) $\gg$ $\Delta H^{\ddagger}$(step IV) and $\Delta S^{\ddagger}$(step III) $\gg$ $\Delta S^{\ddagger}$(step IV). The fact that $\Delta G^{\ddagger}$(step IV) > $\Delta G^{\ddagger}$(step III) at 25 °C accounts for the smaller rate constant and indicates that step IV is entropy-controlled. The extremely small values of $\Delta H^{\ddagger}$ for step IV would under normal conditions suggest a diffusion-controlled process. However, the value of k_{obs} is a composite of rate and equilibrium constants, such that this $\Delta H^{\ddagger}$ value probably results from a large negative ΔH for one or more of the equilibria in reactions 1–7 and 9, combined with a positive value for the actual rate-determining electron-transfer step. The very negative $\Delta S^{\ddagger}$ values for step IV may be in line with the well-ordered structure of dimeric bridged complexes, which could account for the production of $S_2O_6^{2-}$ in argonated solution as well.

Steps III and IV are followed by two further reactions (V and VI) that occur on an hour time scale. At the end of reaction IV, in the absence of oxygen, the solution exhibits an absorption at 280 nm, which is characteristic for SO_2. Under these conditions Fe(III) is reduced to Fe(II) and sulfite is partially oxidized to sulfate and dithionate. During step V, the excess sulfite slowly disappears ($t_{1/2} \approx 30$ min), as judged from the decrease in absorbance at 280 nm (see Figure 8), which is followed by an increase in absorbance at 224 and 304 nm during step VI. The latter increase is ascribed to the formation of Fe^{III}–SO_4^{2-} complexes. The decrease in sulfite concentration (step V) is presumably controlled by the leakage of oxygen into the reaction vessel via tubing used to pump the test solution through the spectrophotometer cell,[2] which also acounts for the final formation of Fe(III). At the end of step VI, all Fe(II) has been oxidized to Fe(III) and addition of sulfite reinitiates the whole process, i.e., steps I–IV. Steps V and VI will not occur under conditions where O_2 is completely absent from the system. An analysis of the reaction products (see Figure 9) during reactions V and VI (no added O_2) clearly indicates a significant increase in the $[SO_4^{2-}]$, whereas the $[S_2O_6^{2-}]$ increases only slightly. This could be due to very low [Fe(III)] during step V (excess of S(IV)), which

(21) Conklin, M. H.; Hoffmann, M. R. *Environ. Sci. Technol.* **1988**, *22*, 899.

(22) Miksztal, A. R.; Valentine, J. S. *Inorg. Chem.* **1984**, *23*, 3548.

(23) Sato, T.; Goto, T.; Okabe, T.; Lawson, F. *Bull. Chem. Soc. Jpn.* **1984**, *57*, 2082.

Table II. Temperature Dependence k_{obs} for Steps III and IV[a]

step	wavelength,[b] nm	T, °C	ΔA[c]	$10^2 k_{obs}$,[d] s^{-1}	$\Delta H^{\ddagger}$, kJ mol^{-1}	$\Delta S^{\ddagger}$, J K^{-1} mol^{-1}
III	390	13.0	−0.486	3.7 ± 0.2	69 ± 8	−30 ± 27
		17.0	−0.456	6.6 ± 0.1		
		25.0	−0.472	13.9 ± 0.4		
		32.6	−0.489	19.0 ± 0.8		
		40.3	−0.447	64.7 ± 0.5		
	470	13.0	−0.206	3.6 ± 0.2	68 ± 7	−32 ± 23
		17.0	−0.204	4.5 ± 0.1		
		25.0	−0.213	13.1 ± 0.1		
		32.6	−0.212	17.4 ± 1.4		
		40.3	−0.202	51.6 ± 0.8		
IV	390	13.0	−0.091	1.09 ± 0.02	8 ± 5	−254 ± 18
		17.0	−0.097	1.19 ± 0.04		
		25.0	−0.060	0.97 ± 0.06		
		32.6	−0.042	1.48 ± 0.06		
		40.3	−0.030	1.61 ± 0.17		
	470	13.0	−0.045	1.05 ± 0.04	13 ± 7	−234 ± 27
		17.0	−0.037	1.17 ± 0.11		
		25.0	−0.030	1.39 ± 0.09		
		32.6	−0.014	1.12 ± 0.24		
		40.3	−0.019	2.32 ± 0.23		

[a] [Fe(III)] = 5×10^{-4} M, [total S(IV)] = 1×10^{-2} M, pH ≈ 2.5, ionic strength 0.1 M, Ar atmosphere. [b] Wavelength at which the reaction was followed. [c] ΔA = absorbance change for a 2-cm path length. [d] Mean value of between four and six kinetic runs.

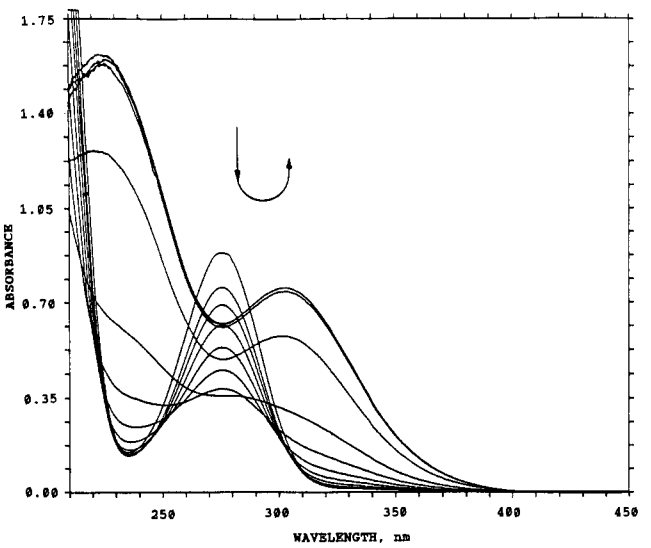

Figure 8. Repetitive-scan spectra for steps V and VI. Conditions: [Fe(III)] = 5×10^{-4} M, [total S(IV)] = 1×10^{-2} M, pH ≈ 2.3, T = 20 °C, Ar atmosphere, Δt = 10 min.

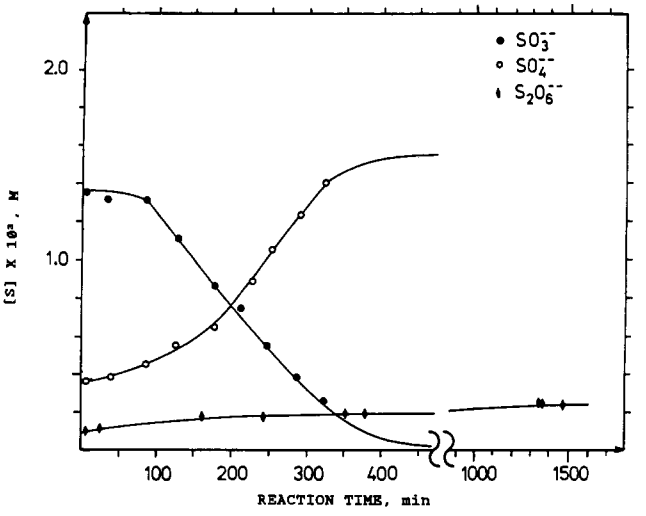

Figure 9. Product distribution of the S–O species during steps V and VI. Conditions: [Fe(III)] = 5×10^{-4} M, [total S(IV)] = 2×10^{-3} M, pH = 3.0–3.5, T = 25 °C, Ar atmosphere.

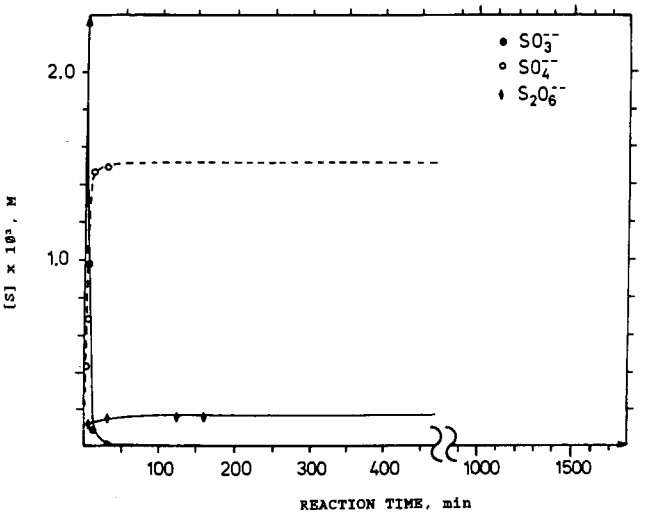

Figure 10. Product distribution of the S–O species during steps V and VI in the presence of O_2. Conditions: [Fe(III)] = 5×10^{-4} M, [total S(IV)] = 2×10^{-3} M, pH ≈ 3.0, T = 25 °C, O_2 atmosphere.

cannot regenerate significant concentrations of the Fe(III) dimer. The produced monomeric Fe(III)–sulfito complexes will most likely lead to SO_4^{2-} production. The concentration of the various sulfur species at $t \approx 0$ corresponds to those reached during steps III and IV of the process. The corresponding results for the process in the presence of O_2 are reported in Figure 10, from which it follows that complete conversion to SO_4^{2-} and $S_2O_6^{2-}$ occurs within less than the first 30 min of the process. The production of dithionate is enhanced by the presence of O_2, although the main product is SO_4^{2-} as also found in Figure 9. Experiments in which sulfate was added to the reaction mixture indicated that the presence of sulfate catalyzed the oxidation of sulfite and suppressed the production of dithionate at high $[SO_4^{2-}]$.

The results reported in this study are of direct significance for environment-related conditions, which will be treated in a subsequent paper.[24] In the remainder of this report we compare the results with available information on the reactivity of transition-metal sulfito complexes.[3-17] It is especially the intramolecular electron-transfer reactions that interest us at present. The O-bonded $Co(NH_3)_5OSO_2^+$ species undergoes electron transfer significantly faster than the corresponding S-bonded species.[3] It is possible that this effect could also account for the difference

(24) Kraft, J.; van Eldik, R. *Atmos. Environ.*, in press.

in redox reactivity observed during steps III and IV of the Fe(III)–S(IV) system. The main redox process occurs during steps III and IIIa, and the main overall oxidation product is SO_4^{2-} with a minor production of $S_2O_6^{2-}$, especially in the presence of O_2. In some of the Pt(IV) and Co(III) systems the redox process exhibits a characteristic pH dependence, which can be interpreted in terms of a more reactive protonated sulfito complex.[9,11,13] A similar effect presumably accounts for the pH dependence of step III as found in this study (see eq 9).

We are not aware of studies on the redox kinetics of bridged metal sulfito complexes that could serve as an appropriate comparison with the reactions suggested to account for step IV of the decomposition process. The oxidation products found in this study, viz. SO_4^{2-} and $S_2O_6^{2-}$, do not exclude the partial formation of $S_2O_7^{2-}$ either as an intermediate or stable product species, as reported in the literature.[25,26] The mechanism for the metal-catalyzed autoxidation in (11), or the mechanism suggested by Conklin and Hoffmann,[21] incorporates the formation of SO_3, which along with SO_4^{2-} could be present in solution as $S_2O_7^{2-}$. In this respect it is important to note that the authors[25,26] conclude from their experiments that $S_2O_7^{2-}$ is formed from one oxygen and two bisulfite molecules and that its formation shows a complicated dependence on trace amounts of metal ions such as Fe^{2+}/Fe^{3+} and Mn^{2+}. In aqueous solution $S_2O_7^{2-}$ can dissociate according to (12), which is similar to the mechanism for the formation of

$$S_2O_7^{2-} + H_2O \rightleftharpoons 2HSO_4^- \qquad (12)$$

HSO_3^- from $S_2O_5^{2-}$. It follows that the mechanistic results of this study may be relevant for the understanding of the formation of $S_2O_7^{2-}$ during the autoxidation of S(IV) oxides.

Acknowledgment. We gratefully acknowledge financial support from the Deutsche Forschungsgemeinschaft, the Fonds der Chemischen Industrie, and the Scientific Affairs Division of NATO under Grant No. RG. 0681/85. Drs. M. R. Hoffmann and M. H. Conklin are thanked for providing preprints of their papers prior to publication. We acknowledge the kind assistance of Dr. Achim Gerhard (Max Planck Institute for Biophysics, Frankfurt, FRG) with some of the spectroscopic measurements and Dr. W. Jaeschke (Zentrum für Umweltforschung, University of Frankfurt) for some preliminary ion chromatographic analyses.

Registry No. O_2, 7782-44-7.

(25) Chang, S. G.; Littlejohn, D.; Hu, K. Y. *Science* **1987**, *237*, 756.
(26) Littlejohn, D.; Hu, K. Y.; Chang, S. G. *Ind. Eng. Chem. Prod. Res. Dev.* **1988**, *27*, 1344.

Contribution from the Department of Chemistry, University of Miami, Coral Gables, Florida 33124

Synthesis and Reactivity of Pyridine *N*-Oxide Complexes of Cobalt(III)

William L. Purcell

Received July 6, 1988

The syntheses of four new pentaamminecobalt(III) complexes with pyridine *N*-oxide, 4-methylpyridine *N*-oxide, 2-cyanopyridine *N*-oxide, and 4-cyanopyridine *N*-oxide are described. The first two ligands bond through the oxygen, while the latter two ligands are bonded via the nitrile group nitrogen. Reaction kinetics have been used to investigate the reactivity of these complexes. The rate constant for aquation of the pyridine *N*-oxide complex at 25 °C is 2.51×10^{-6} s^{-1}. Chromium(II) reduction of the pyridine *N*-oxide complex is an inner-sphere process with a rate constant at 25 °C of 0.371 M^{-1} s^{-1}, an activation enthalpy of 3.75 ± 1.2 kcal mol^{-1}, and an activation entropy of −48 ± 4 cal K^{-1} mol^{-1}. The 4-cyanopyridine *N*-oxide complex undergoes facile base hydrolysis of the nitrile function to a bound amide. The rate constant for this process at 25 °C is 4030 ± 125 M^{-1} s^{-1}. The 2-cyanopyridine *N*-oxide complex exhibits this same nitrile group conversion even in *acidic* solution, where water is shown to function as a competitive attacking nucleophile.

Introduction

Few cobalt(III) amine *N*-oxide complexes have been reported, in sharp contrast to the large number of complexes known with other transition metals.[1-5] Nathan et al. described the synthesis of three Co(III) complexes with bidentate ligands containing at least one amine *N*-oxide function in 1979[6] and offered several reasons for the dearth of other examples. Among these were the weak donor properties of the *N*-oxide function and the difficulty of nonaqueous oxidation of Co(II) precursors. Hence, most examples of *N*-oxide complexes utilize chelating ligands.[6-9] Indeed, the only example of a monodentate amine *N*-oxide complex appears to be the *trans*-bis(diethylglyoximato)cobalt(III) pyridine *N*-oxide complexes reported by Ablov et al.[10] This article reports the facile, high-yield synthesis of both pentaammine(pyridine *N*-oxide)cobalt(III) and complexes with substituted pyridine *N*-oxides. The reactivity of these complexes is also reported via kinetic studies of aquation, electron transfer by chromium(II) reduction, and ligand reactivity.

Experimental Section

Materials. Pyridine *N*-oxide from Aldrich Chemical Co., Inc., and 4-methylpyridine *N*-oxide from Eastman Organic Chemicals were recrystallized from toluene before use. 2- and 4-cyanopyridine *N*-oxides were prepared from their cyanopyridines (Aldrich) by the method of Ochiai.[11] Literature methods were employed to prepare $[Co(NH_3)_5N_3](ClO_4)_2$[12] and $[Co(NH_3)_5OSO_2CF_3](CF_3SO_3)_2$ ("cobalt triflate").[13] Solvents for synthetic procedures were dried over 4-Å molecular sieves before use.

House-supplied distilled water was deionized through an Illinois Water Treatment Universal Model 2 resin cartridge for kinetic studies. Sodium perchlorate (G. F. Smith Chemical Co.) stock solutions for ionic strength

(1) Garvey, R. G.; Nelson, J. H.; Ragsdale, R. O. *Coord. Chem. Rev.* **1968**, *3*, 375.
(2) Orchin, M.; Schmidt, P. J. *Coord. Chem. Rev.* **1968**, *3*, 345.
(3) Karayannis, N. M.; Pytlewski, L. L.; Milkulski, C. M. *Coord. Chem. Rev.* **1973**, *11*, 93.
(4) Karayannis, N. M.; Speca, A.; Chasan, D. H.; Pytlewski, L. L. *Coord. Chem. Rev.* **1976**, *20*, 37.
(5) Giesbrecht, E. *Pure Appl. Chem.* **1979**, *51*, 925.
(6) Nathan, L. C.; Armstrong, J. E.; Ragsdale, R. O. *Inorg. Chim. Acta* **1979**, *35*, 293.
(7) Lever, A. B. P.; Lewis, J.; Nyholm, R. S. *J. Chem. Soc.* **1962**, 5262.
(8) Robinson, M. A. *J. Inorg. Nucl. Chem.* **1964**, *26*, 1277.
(9) Summers, J. T.; Quagliano, J. V. *Inorg.* Chem. **1964**, *3*, 1767.
(10) Ablov, A. V.; Batyr, D. G.; Starysh, M. P. *Russ. J. Inorg. Chem.* (*Engl. Transl.*) **1971**, *16*, 368.
(11) Ochiai, E. *J. Org. Chem.* **1953**, *18*, 534.
(12) Balahura, R. J. *Can J. Chem.* **1974**, *52*, 1767.
(13) Dixon, N. E.; Jackson, W. G.; Lancaster, M. J.; Lawrence, G. A.; Sargeson, A. M. *Inorg. Chem.* **1981**, *20*, 470.

0020-1669/89/1328-2312$01.50/0